On the Magnitude of the Electric Field Near Thunderstorm-Associated Clouds

Francis J. Merceret[*]

Jennifer G. Ward[*]

Douglas M. Mach[#]

Monte G. Bateman[&]

James E. Dye[+]

[*] National Aeronautics and Space Administration/Kennedy Space Center, FL

[#] University of Alabama, Huntsville, AL

[&] Universities Space Research Association, Huntsville, AL

[+] National Center for Atmospheric Research, Boulder, CO

Corresponding Author: Francis J. Merceret, NASA/YA-D, Kennedy Space Center, FL 32899,

Phone 321-867-0818, fax 321-867-3720, email francis.j.merceret@nasa.gov.

Co-author contact information:
Ward - NASA/YA-D, Kennedy Space Center, FL 32899,
Phone 321-867-0824, fax 321-867-3720, email jennifer.g.ward@nasa.gov.

Mach - Earth Systems Science Center, University of Alabama, GHCC, 320 Sparkman Dr., Huntsville, AL 35805, Phone 256-961-7830, email dmach@ nasa.gov.

Bateman - Universities Space Research Association, 320 Sparkman Dr., Huntsville, AL 35805, Phone 256-961-7804, email monte.bateman@ nasa.gov.

Dye - NCAR, POB 3000, Boulder, CO 80307, Phone 303-497-8944, email dye@ucar.edu

[This draft 10 January 07 for final review by coauthors before submission to JAM. Incorporates responses to 07 Nov 06 draft and changes due to lightning in ABFM-II clouds.]

ABSTRACT

Electric field measurements made in and near clouds during two airborne field mill programs are presented. Aircraft equipped with multiple electric field mills and cloud physics sensors were flown near active convection and into thunderstorm anvil and debris clouds. The magnitude of the electric field was measured as a function of position with respect to the cloud edge in order to provide an observational basis for modifications to the lightning launch commit criteria (LLCC) used by the U.S. space program. These LLCC are used to reduce the risk that an ascending launch vehicle will trigger a lightning strike that could cause the loss of the mission or vehicle. The results suggest that even with fields of tens of kV m^{-1} inside electrically active convective clouds, the fields external to these clouds decay to less than 3 kV m^{-1} within fifteen kilometers of cloud edge. Fields exceeding 3 kV m^{-1} were not found external to anvil and debris clouds.

1. Introduction

This paper presents measurements of electric fields aloft in and near clouds associated with thunderstorms. The emphasis is on thunderstorm anvil and debris clouds associated with the decaying phase of thunderstorms. An excellent summary of published measurements of thunderstorm electric fields aloft through the mid-1990s may be found in Chapter 7 of MacGorman and Rust (1998). Nearly all of those measurements were made in cloud and most were taken during the growth or mature stage of the storms.

Electric fields in or near anvils and debris clouds is of concern to aviation and aerospace interests because of the threat of triggered lightning. Air and spacecraft completely avoid flight through active convection because of the multiple threats of natural and triggered lightning, wind shear, turbulence and hail. Anvils and debris clouds produced by thunderstorms cover much more airspace and can persist longer than the convective cores that produce them. Unconditional avoidance of all such clouds would unnecessarily cause delays or diversions of air traffic and delays or scrubs of aerospace launch and landing operations. On the other hand, even in the absence of natural lightning, lightning may be triggered in or near such clouds if the electric fields are high enough. Triggered lightning has destroyed both aircraft and space vehicles. An excellent summary of the matter is found in Chapter 10 of Rakov and Uman (2003).

For space launches, NASA and the U.S. Air Force developed a set of lightning launch commit criteria (LLCC) to protect vehicles from natural and triggered lightning during ascent. These LLCC prohibit flight through or close to specific types of clouds

including anvil and debris clouds depending on the optical and radar properties of the clouds and the time of occurrence of the last lightning in the cloud or its parent thunderstorm. Specific stand-off distances and waiting times are provided. Details may be found in Willett *et al.* (1999). These rules are safe but can be quite restrictive. In the early 1990s NASA conducted an airborne field mill (ABFM) program [hereafter referred to as ABFM-I] to measure electric fields aloft in and near thunderstorm-related clouds to determine if the LLCC could be safely relaxed. A second ABFM program, ABFM-II, was conducted during 2000 and 2001. The two programs were similar overall, but the objectives differed significantly. ABFM-I is described in Christian *et al.* (1993). ABFM-II is described in Merceret and Christian (2000) and Dye *et al.* (2004, 2007).

This paper presents the results of one aspect of these ABFM efforts: the decrease in magnitude of the electric field with distance from cloud edge. If it could be shown that the electric field, which may be tens or even hundreds of kV m^{-1} in cloud, becomes small (< 3 kV m^{-1}) at a short distance outside the cloud, then the standoff distances in the current LLCCs may be safely reduced. Section 2 of the paper describes ABFM-I and its results. Section 3 describes ABFM-II and its results. Section 4 discusses the common findings, differences and implications of the two programs.

2. ABFM-I

a. Description

The ABFM-I program consisted of 4 deployments to the KSC area with two deployments during summer and two during winter conditions found in Florida near

KSC. The summer goals included determining when developing cumulus become a hazard to launch vehicles, how far away from mature clouds the hazardous fields extend, and when the thunderstorm debris clouds are no longer a hazard to launch vehicles. The main winter target was layered clouds. The winter goals included determining at what overall thickness layered clouds (including but not limited to altostratus and cirrostratus) become a hazard to launch vehicles and were there other measurements of how to determine if a layered cloud was, or was not, a hazard. In addition, all deployments were used to test the ability of a network of 31 ground-based field mills (GBFM) at KSC and Cape Canaveral Air Force Station to detect electrically hazardous conditions aloft. The first summer deployment was in July and August 1990 and consisted of 31 data flights. The first winter deployment was in February and March 1991 and had 18 data flights. The second summer deployment was in July and August 1991 and also had 31 data flights. The second winter deployment was in January through March 1992 and had 25 data flights.

The ABFM-I data presented in this paper were collected in the vicinity of actively growing cumulus or thunderstorms. In contrast, the data collected during ABFM-II, described in the next section, were from decaying thunderstorm anvils or debris clouds. One of the consequences is that the "screening layer" that can form on the outside of cloud is expected to be absent or only weakly present in the ABFM-I target clouds. Charge in the interior of a cloud attracts charge of the opposite sign from the surrounding air. At the cloud boundary, the relatively high conductivity of the clear air gives way to the lower conductivity of the cloudy air. Thus, the attracted charge tends to accumulate at the edges of the cloud. If the cloud is growing, that charge layer gets entrained into the

cloud and diluted or neutralized. Vonnegut *et al.*, 1966, present measurements demonstrating this at the upper cloud boundary. If the cloud is not growing, the attracted charge accumulates on the boundary of the cloud. Outside of the cloud, the field due to this screening layer tends to cancel the field caused by the charge in the cloud interior. That may be one reason why the data show stronger fields outside of the clouds in ABFM-I than for those in ABFM-II, although further research is clearly required since the evidence for horizontal screening layers is weak at best (Dye *et al.*, 2006)

For ABFM-I, target clouds were first identified with radar. If the target was a growing cumulus, the aircraft was then directed to fly at the top of the growing cloud (just penetrating the top edge of the cloud). If the target was a mature cumulus, the aircraft was directed to fly towards the cloud and then turn away either at the edge or further out from the cloud (depending on the severity of the target). In all cases, the aircraft was to avoid areas with known lightning or reflectivity values of 30 dBz or more based on returns from the on-board radar.

b. Instrumentation

The aircraft used was a Lear 28/29 (experimental hybrid) business jet, operated by NASA/Langley Research Center. The aircraft carried 5 rotating-vane type electric field mills and a data collection system consisting of a PC-AT computer with Exabyte tape recorder. The data were also telemetered to ground and recorded there.

The Lear 28/29 carried a liquid water content (LWC) King probe, made by Particle Measurement Systems (PMS). It also had a "charging patch" [Davis *et al.*

(1989)] that sensed the presence of ice crystals by differential charging. Combining these two gave indications that the aircraft was flying in liquid, mixed-phase, or ice clouds. Additionally, pilots were tasked with noting entry into and exit from cloud as accurately as possible. The charging patch was used to distinguish ice clouds from those without ice.

Volume scan reflectivity data were available from the WSR-74C weather radar located at Patrick Air Force Base, FL. This is a C-band (5.3 cm) horizontally polarized conventional weather radar. Because of calibration issues during ABFM-I, this radar could not be used quantitatively to relate measured electric fields to radar reflectivity, but it was useful for characterizing the general environment in which the data were taken. Despite the calibration uncertainties, the measured values are believed to be close to the true values.

There was also a small lightning ground-strike location system installed at KSC, and it was used to warn the pilots away from storms with lightning. A more detailed description of all of the instrumentation for ABFM-I may be found in Fisher *et al.* (1992).

c. Data Analysis

The five field mills on the aircraft were first calibrated in the laboratory to determine the basic instrument calibration constant that converts output voltage to electric field. Once the mills were mounted on the aircraft, the aircraft was directed to perform a series of roll and pitch maneuvers at low altitude under fair weather conditions. Since the fair weather field is vertical and reasonably known, the roll and pitch maneuvers rotated the predominantly vertical field (Ez) into the other components (Ex

and Ey). By manually examining the various mill responses to the roll and pitch maneuvers, a relative calibration relationship (or matrix) between the mill outputs and the external electric field was determined. A high voltage "stinger" was used to charge the aircraft to determine the final relative calibration. A series of fly-bys of a calibrated ground based field mill provided the final absolute calibration.

The data were monitored in real-time on the ground and on the aircraft. Each field mill produced a periodic calibration pulse used to monitor the health and calibration of the field mill. Any problems with the mills or the calibrations were noted in the data logs. The real-time telemetered data were recorded on the ground on Exabyte tapes and the data recorded on the aircraft was transferred to Exabyte tape in the same format for archive.

During ABFM-I, the cloud edge was determined manually using three methods: (1) Pilot report (visually), (2) 2 dBZ radar echo, and (3) liquid water content (LWC) probe or charge patch. The mean and standard deviation of the magnitude of the electric field outside of the cloud was determined as a function of distance from cloud edge. No attempt was made to determine the variation of the fields inside the cloud as a function of cloud edge distance.

d. Results for Developing Cumulii

For ABFM-I, 43 developing cumuli were sampled in 1990 and 44 in 1991. The results indicated that the observed electric fields depended strongly on the cloud top

height as defined by the uncalibrated 10 dBZ reflectivity. Fields in clouds with 10 dBZ tops lower than the 0°C level did not exceed 3 kV m^{-1}.

Clouds with tops between 0°C and −10°C sometimes had fields greater than 1 kV m^{-1}. There were three cases where a cloud was very near the −10°C level and growing rapidly that had fields greater than 3 (but less than 5) kV m^{-1}. However the vast majority of the clouds in this range had fields less than 1 kV m^{-1}

Fields greater than 3-5 kV m^{-1} did not develop in the clouds until the echo top of the cloud had grown higher than the −10°C level (average altitude 6.4 km above mean sea level). Furthermore, the study clouds did not produce lightning until the tops were higher than the −20°C level. Fields at the edge of clouds with echo tops higher than the −20°C level could be greater than 50 kV m^{-1}.

Figure 1 shows the average and peak electric field magnitudes for ABFM-I approaches to active convection as a function of distance from cloud edge. If the cloud was not penetrated by the aircraft (due to lightning or excessive fields), the uncalibrated 2 dBZ echo edge was used as the cloud boundary. Some of these clouds were associated with storms that were producing lightning at the time the measurements were taken. Penetrations with and without lightning were averaged separately and also combined. Peak values are shown only for the separate cases since the combined case is merely the maximum of the separate cases.

For these actively growing storms, the magnitude of the electric field was reliably below the 3 kV m^{-1} threshold for distances larger than 15 km. Even in clouds with tops above −20°C, the maximum fields dropped off to less than 3 kV m^{-1} by 8 km from the edge of the cloud in the absence of lightning. In most cases, the fields decayed much

quicker than these values. The average value was below the threshold beyond 6 km even for storms actively producing lightning.

3. ABFM-II

a. Description

The ABFM II campaigns were conducted during June 2000 and May-June 2001 to obtain ground-based radar measurements simultaneously with airborne measurements of the electric fields, and microphysical content in anvils, thick clouds, and debris clouds near Kennedy Space Center. Flights of the Univ. of North Dakota Citation II jet aircraft were coordinated with the WSR74C 5-cm radar at Patrick Air Force Base, which was well calibrated for ABFM-II, and the 10-cm WSR88D radar at Melbourne, Florida. When possible, flights were conducted over the ground based field mill (GBFM) network at KSC and in the operating range of the KSC Lightning Detection and Ranging (LDAR) system and the Cloud to Ground Lightning Surveillance System (CGLSS).

During the campaign, initial anvil penetrations were typically made near to and somewhat downstream from the convective cores of storms. Then subsequent passes were made across the anvil at different distances downstream to examine the decay of the electric field both with time and distance. Anvils were sampled during 19 flights at a wide variety of altitudes in different locations relative to anvil top and bottom and relative to distance from the storm core. There is enough variety in these measurements to be representative of conditions in anvils of Florida thunderstorms. Various flight plans were used to sample the cloud as a function of distance (which corresponds to translation time) from the core. Some flights were made across the anvil, with each subsequent pass at a higher or lower altitude in stair step fashion. Some flights were made along the

downwind axis of the anvil to measure electric field vs. the translation time (*i.e.* time for electric field to decay) at different positions in the downwind anvil. Some flights were made after convection in the core had ceased and the anvil was dissipating but while enhanced electric fields still existed. Decisions on where to fly were interactive between crew in the aircraft and aircraft coordinators at the KSC Range Operations Control Center (ROCC).

A critical measurement from the aircraft was the in-situ measurement of the 3-dimensional electric field. This was accomplished using 6 high sensitivity, low noise electric field mills described in Section 3.b below. The microphysical observations were made with several different instruments also described in Section 3.b. Information on the University of North Dakota Citation II jet aircraft operating characteristics and the instruments flown during ABFM II can be found in Appendices of Dye *et al.* (2004, 2006) The Citation II had an operating ceiling of 13.1 km. It could cruise at speeds of up to 175 m s^{-1} and climb at 16.8 m s^{-1} with an on-station time of up to 4 hours depending on mission type. It could safely be flown at speeds as low as 72 m s^{-1} when necessary for some kinds of measurements.

b. Instrumentation

The rotating-vane field mills flown during ABFM-II were designed and built by NASA/MSFC. These mills are described in detail in Bateman et al. (2006). Six mills were used to assure adequate data to resolve the vector components of the field plus the field due to charge on the aircraft, and some redundancy for data quality control. The data collection system was a Pentium-class PC. A GPS card was used to keep the data time-synchronized to UTC. The computer synchronizes the data collection for each mill and

also records the data that the mill sends back. The field data were displayed in real time, which was used to advise the pilot on safety.

ABFM-II used volume scan reflectivity data from the same WSR-74C weather radar located at Patrick Air Force Base, FL that was used for ABFM-I. However, for ABFM-II this radar was calibrated within +/- 1 dBZ and could be used quantitatively. In addition, ABFM-II also used "Level 2" volume scan reflectivity data from the WSR-88D NEXRAD radar at Melbourne, FL (KMLB). Comparisons of measurements from the two radars for a few times and storms showed agreement within 2 to 3 dBZ when attenuation of the 5 cm WSR-74C was not an issue.

ABFM-II used lightning location information from two sources: Lightning Detection and Ranging (LDAR) operated by NASA at Kennedy Space Center (KSC), and the Cloud to Ground Lightning Surveillance System (CGLSS) operated by the Air Force at the Eastern Range. CGLSS provides the location of the return strokes of cloud to ground lightning with an accuracy (circular error probability of 50%) of 300 m within 40 km of the center of the network near KSC. The accuracy degrades to 3 km at a distance of 100 km. The detection efficiency is greater than 90%. LDAR locates the three-dimensional path of each flash with an accuracy of 100m within 10 km of the center of the network at KSC and 1 km to a range of 100 km. The detection efficiency exceeds 90%. The advantage of LDAR is that it locates in-cloud lightning as well as cloud to ground lightning. Additional information on both systems may be found in Maier *et al.* (1995). As with ABFM-I, lightning data were used for flight safety. They were also used during

analysis to determine the time and distance of the last lightning flash either in the cloud being penetrated or one nearby.

During ABFM-II particle measurements were made with five different particle probes that spanned particle sizes from a few microns to about 5 cm, thus from frozen cloud droplets to very large aggregates. To determine cloud edge, the primary microphysical instruments were the Particle Measuring Systems (PMS) Optical Array 2D Cloud (2D-C) probe with a range of ~ 30 μm to a few mm; [See Strapp *et al.* (2001) for a recent discussion of the 2D-C probe], the PMS Optical Array 1D Cloud (1D-C) probe with a range from 20 to 600 μm, and the PMS Forward Scattering Spectrometer Probe (FSSP) with range for water droplets of ~3 to 50 μm [Dye *et al.* (1984)]. Although the community has used the FSSP primarily for the measurement of cloud droplets it also is effective at detecting ice particles, but sizing is inaccurate and the measured concentrations are overestimates due to particles shattering on the probe tips, especially in broad ice particle spectra such as those we found in Florida anvils. See Field *et al.* (2003) for a discussion of this problem. It was not a primary instrument for detecting cloud edge in this study because spurious counts often appeared in the smaller size bins even out of cloud.

Each of the particle instruments was calibrated using standard calibration techniques. The measurements from these probes were processed and displayed using software developed at the National Center for Atmospheric Research. Data from each of these sensors were processed to produce size distributions for each probe averaged over ten second time periods. The agreement between the 1DC and the 2DC in the region of

overlap was in general very good except for the smallest sizes where the instrument response was an issue and the largest sizes where the sample sizes are small (See Dye *et al.*, 2006). In most circumstances the entries into or exits from cloud determined from the individual instruments agreed quite well.

c. Data Analysis

Analysis of ABFM II data was based on composite files created for each flight by merging measurements from airborne, surface and radar sources. The instruments used to make these measurements were carefully calibrated and quality controlled. These merged files contained 10 s averages of time synchronized aircraft measurements including electric fields and particle measurements with the corresponding radar reflectivity measurement for the location and altitude of the aircraft at that time. For the nominal speed of the aircraft of 120 m/s, 10 s corresponds to approximately 1.2 km of flight track and is roughly equivalent to the 1 km gridding of the radar data. These merged files contained radar observations from both the WSR74C and NEXRAD WSR88D radars. An example of a graphical display showing both radar and airborne measurements generated from a merged data set is presented in Figure 2.

The merged data files were used extensively for a number of different studies over a 2 year period following the field campaigns. During the analysis, an occasional timing error or other problem became apparent. As problems were found, corrections were made to the data set and files. This data set is now quite mature, of high quality, and unlikely to contain errors that would impact the present study. It is archived at http://abfm.ksc.nasa.gov. To access the KSC site, a user id and password must be

obtained from the supervisor of the Cape Canaveral Joint Base Operations Center at the CARE Center, 321-867-5010 or CARECenter@jbosc.ksc.nasa.gov.

For the results presented in this paper we have included only those measurements that were made in close proximity to or inside anvils or debris clouds. To be considered an anvil for this analysis, a cloud must have the morphological structure of an anvil: *i.e.* it was produced by a downshear or upshear outflow or blow-off from an active cumulus convective core and had a well-defined base. The convective core may either still exist at the time of the penetration or could have decayed, *i.e.* the anvil can be attached or detached. This requires determining the previous history of the cloud in question. Decay products left in place at higher altitudes from once active convective cores growing in a low shear environment are NOT considered to be an anvil, but for the purpose of this paper are referred to as debris clouds.

In contrast to the strategy and results obtained from ABFM-I, where the focus tended to be on the core of developing cumuli or on approaching the cloud edge of the core of active mature storms, the emphasis in ABFM-II was on measurements in anvils and debris clouds mostly away from storm cores. The flight strategies and subsequent data classification of ABFM-I and ABFM-II were very different. Consequently the results obtained from the two projects were also different. There are similarities in that the electric fields fall off rapidly from cloud edge for both data sets, but the magnitude of the field is larger near the growing and active clouds of ABFM-I.

Because of the large amount of data and the tediousness of manual analysis, the distance from cloud edge for ABFM-II was computed automatically. The position of the cloud edge was determined using the algorithm described by Ward and Merceret (2004).

It determines whether the aircraft is in or out of cloud based primarily on 2DC cloud particle measurements or, under certain conditions, 1 DC measurements and radar data. Cloud edges are determined from transitions between in and out of cloud subject to a hysteresis constraint.

The distance from the identified cloud edge was computed based on the aircraft speed and three assumptions about the flight track. The aircraft flew at a nominal speed of 120 m s^{-1} and so each ten second record was assumed to represent 1.2 km of travel horizontally. The other assumptions were that the flight track was essentially perpendicular to the cloud edge and that there were no underlying or overhanging clouds closer to the aircraft than the computed horizontal distance from the cloud. The perpendicularity assumption was generally valid since the flight tracks were selected to transect the cloud across or along its major axis. The assumption about clouds overhanging or underlying the aircraft was frequently invalid, and these cases had to be detected and eliminated as described in the next paragraph.

The automated algorithm provided a list of the date and time of each cloud entry and exit it detected. The radar cross sections along the flight track such as the example shown in the MER plot in Figure 2 were examined for each case to ensure that the assumption discussed above was valid. Entries or exits with significant underlying or overhanging cloud were eliminated from the analysis since the distances from cloud edge generated in the statistical data base were invalid. A typical example of an invalid entry is shown in Figure 3. Here the aircraft flew less than 1 km below cloud base but outside of the cloud as determined by both cloud physics and radar data for 50 seconds before entering the cloud. The fields measured during those 50 seconds would be reported as

fields at distances ranging from 1 to 6 km rather than at their actual distance if this case were kept in the data base.

For the ABFM-II data, the maximum, mean and other statistics of the electric field magnitude were computed as a function of distance from cloud edge. Anvil and debris cloud were treated separately to determine if the results significantly differed. Since only fields of 3 kV m^{-1} or greater were considered hazardous for our purposes, the analysis excluded cases where the maximum field magnitude within the cloud was less than that value. Inclusion of fields associated with non-hazardous clouds would reduce the average and median values, thus providing a false indication of the actual threat in the vicinity of strongly electrified clouds.

d. Results

Maximum and average values of the magnitude of the electric field as a function of distance from cloud edge are shown for anvils and debris cloud respectively in figures 4 and 5. These are based on 18 anvil and 11 debris cloud penetrations. The statistical sampling error in Fig. 2 is 120 V m^{-1} from the cloud edge outward and rises to a maximum of 3.8 kV m^{-1} in the high field portion of the interior of the cloud. The corresponding sampling errors for Fig. 5 are 182 V m^{-1} and 6.5 kV m^{-1}. The behavior is very similar. The field magnitudes drop below the hazard threshold of 3 kV m^{-1} inside the cloud before the edge is reached in both anvil and debris clouds even in the worst case. Fields below this threshold are believed not to pose a threat that a launch vehicle will trigger lightning (See Willett *et al.*, 1999). The average fields outside the cloud do not exceed 1 kV m^{-1} right up to cloud edge.

The figures also show that the debris clouds had generally larger fields than anvils in the cloud interiors but from the cloud edge outward, the fields near anvil and debris clouds behaved almost identically. This suggests that in determining safe external stand-off distances for LLCC, anvil and debris clouds may be treated in the same manner.

4. Discussion

In contrast with the ABFM-I results in clouds associated with active storms exhibiting charge production and lightning, the maximum fields measured during ABFM-II fell below hazardous levels everywhere outside of the cloud even when the fields several km inside the cloud were tens of thousands of volts per meter. Figure 6 presents the average and peak field magnitudes for both experiments as a function of distance from the cloud edge. The ABFM-II anvil and debris data are combined in this figure since they are so similar. To combine the data in the most conservative (safe) way from the point of view of application to LLCC development, at each distance, the larger of the anvil or debris statistic was plotted for comparison with ABFM-I. The ABFM-I max data in the figure were not dominated by a single case. Of 60 cases, 16 had high fields at cloud edge.

The data suggest that cumulus clouds associated with active, charge producing thunderstorms may produce external electric fields exceeding 3 kV m^{-1} up to as much as 15 km from cloud edge. Conversely, when only anvil or debris clouds are considered, the external field magnitude is benign right up to the cloud edge even with large fields in the cloud interior.

The observations reported here may permit some relaxation of the stand-off distances in the operational LLCC for anvils of the type penetrated in ABFM-II.

Depending on the rule, these distances are currently set at 9.26 km (5 nmi) or 18.52 km (10 nmi). If these distances could be reduced significantly with appropriate constraints regarding active storms, the number of unnecessary launch scrubs and delays due to violation of the LLCC could be proportionately reduced. The cost savings could be substantial at those launch sites where the threat of triggered lightning is a major concern.

Clouds of the type penetrated in ABFM-I produce potentially hazardous fields at distances large enough to suggest that little if any reduction in the stand-off distances in the LLCC may be advisable for these clouds.

ACKNOWLEDGMENTS

The authors thank Tony Grainger and his team of scientists, engineers and pilots at the University of North Dakota (UND) for their outstanding support with the UND Citation aircraft and instrumentation. We also thank Sharon Lewis and Mike Dye of the National Center for Atmospheric Research (NCAR) for creating and maintaining the NCAR data archive facility for the ABFM-II program. Funding for this project was provided by the National Aeronautics and Space Administration and the Department of Defense.

Mention of a proprietary product or service does not constitute an endorsement thereof by the authors, their institutions or the American Meteorological Society.

REFERENCES

Bateman, M.G., M.F. Stewart, R.J. Blakeslee, S.J. Podgorny, H.J. Christian, D.M. Mach, J.C. Bailey, D. Daskar, and A.K. Blair, 2006: A low noise, microprocessor-controlled, internally digitizing rotating-vane electric field mill for airborne platforms, accepted by *J. Atmos. Oceanic Technol.*

Christian, H.J., D.M. Mach and J.C. Bailey, 1993: The Airborne Field Mill Project: A Program Summary, A32E-03, EOS Transactions, Vol. 74, No. 43, October 26, 1993, Supplement.

Davis, R.E., D.V. Maddalon, R.D. Wagner, D.F. Fisher and R. Young, (1989): Evaluation of Cloud Detection Instruments and Performance of Laminar-Flow Leading-Edge Test Articles During NASA Leading Edge Flight-Test Program, NASA Tech. Paper TP-2888, April 1989. Available from NASA Center for AeroSpace Information (CASI), 7121 Standard Drive, Hanover, MD 21076-1320.

Dye, J.E., M.G. Bateman, H.J. Christian, E. Defer, C.A. Grainger, W.D. Hall, E.P. Krider, S.A. Lewis, D.M. Mach, F.J. Merceret, J.C. Willett and P.T. Willis, 2007: Electric Fields, Cloud Microphysics and Reflectivity in Anvils of Florida Thunderstorms, accepted by *J. Geophys. Res.*

Dye, J. E., and D. Baumgardner, 1984: Evaluation of the forward scattering spectrometer probe. Part I: Electronic and optical studies. *J. Atmos. Ocean Tech.*, **1**, 329-344.

Dye, J.E., S. Lewis, M.G. Bateman, D.M. Mach, F.J. Merceret, J.G. Ward and C.A. Grainger, 2004: Final Report on the Airborne Field Mill Project (ABFM) 2000-2001 Field Campaign, NASA/TM-2004-211534, National Aeronautics and Space Administration, Kennedy Space Center, FL, 132 pp. Available from NASA Center for AeroSpace Information (CASI), 7121 Standard Drive, Hanover, MD 21076-1320.

Field, P.R., Wood, R., Brown, P.R.A., Kaye, P.H., Hirst, E., Greenaway, R., Smith, J.A., 2003: Ice particle interarrival times measured with a fast FSSP, *J. Atmos. Ocean Tech.*, **20(2)**, 249-261.

Fisher, B.D., M.R. Phillips and L.M. Maier, 1992: Joint NASA/USAF Airborne Field Mill Program – Operational and Safety Considerations During Flights of a Lear 28 Airplane in Adverse Weather, Paper AIAA-92-4093, 6th AIAA Biennial Flight Test Conference, 24-26 August 1992, Hilton Head, SC.

MacGorman, D.R. and W.D. Rust, 1998: *The Electrical Nature of Storms*, Oxford University Press, NY, NY, 422 pp.

Maier, M.W., L.M. Maier and C. Lennon, 1995: Lightning detection and location systems for spacelift operations. Preprints, *Sixth Conference on Aviation Weather Systems*, American Meteorological Society, Dallas, TX, January 15-20, 1995, 292 - 297.

Merceret, F.J. and H. Christian, 2000: KSC ABFM 2000 - A Field Program to Facilitate Safe Relaxation of the Lightning Launch Commit Criteria for the American Space Program, Paper # 6.4, 9th AMS Conference on Aviation and Range Meteorology, Orlando, Florida, 11-15 September 2000.

Rakov, V.A. and M.A. Uman, 2003: *Lightning: Physics and Effects*, Cambridge University Press, 687 pp.

Strapp, J.W., Albers, F., Reuter, A., Korolev, A.V., Maixner, U., Rashke, E. and Vukovic, Z., 2001: Laboratory measurements of the response of a PMS OAP-2DC, *J. Atmos Ocean. Tech,* **18(7)**, 1150-1170.

Vonnegut, B., C.B. Moore, R.P. Espinola, H.H. Blau, Jr., 1966: Electric Field Potential Gradients above Thunderstorms, *J. Atm.. Sci.*, **23**, 764-770.

Ward, J.G. and F.J. Merceret, 2004: An Automated Cloud-Edge Detection Algorithm Using Cloud Physics and Radar Data, *J. Atm. & Ocean. Tech.,* **21(5)**, 762-765.

Willett, J.C., H.C. Koons, E.P. Krider, R.L. Walterscheid, and W.D. Rust, 1999: Natural and Triggered Launch Commit Criteria (LLCC), Aerospace Report A923563, Aerospace Corp., El Segundo, CA, 23pp.

FIGURE CAPTIONS

Figure 1. Electric field magnitude for ABFM - I as a function of distance from the edge of actively growing storms. In the legend, "Avg" denotes the average and "Max" denotes the peak magnitude of the field. "WithLtng" denotes storms with active lightning and "NoLtng" denotes those without active lightning at the time of sampling. The "Combined" curve includes all storms without regard for the presence of active lightning at the time of sampling.

Figure 2. Typical microphysics, electric field and radar (MER) plot. The top panel shows cloud particle concentrations from the 1D, 2D and FSSP instruments. The second panel presents ground-based radar reflectivity along with the air temperature at the aircraft position plus the aircraft bank angle. The third panel is a time height presentation of ground-based radar reflectivity in a plane containing the aircraft track from the ground to the top of the radar scan. The bold line is the aircraft track. The bottom panel presents electric field components measured at the aircraft. The bold line is the scalar magnitude. The thin line is the vertical component and the dotted line is the field due to charge on the aircraft.

Figure 3. Radar panel of microphysics, electric field and radar (MER) plot for 24 June 2001, 1830 to 1840 UTC. Data are from the Melbourne (KMLB) WSR-88D (NEXRAD). The panel presents a vertical cross section of the reflectivity (dBZ) along the aircraft flight track. The vertical axis is altitude (km). The horizontal axis is time (UTC): each major tick represents one minute. The aircraft position is given by the solid black

line near 9 km altitude. It entered the anvil one major tic to the right of center at 1835:50, but was flying less than 1 km below cloud base beginning at 1835:00 at the center of the figure.

Figure 4. Electric field magnitude as a function of distance from the edge of ABFM-II anvil clouds having a maximum field magnitude of at least 3 kV m^{-1}. The maximum and average values are shown separately for passes entering cloud and exiting cloud. The hazard threshold of 3 kV m^{-1} is shown by a horizontal dashed line. The cloud boundary is at the midpoint of the chart (distance = 0) with cloud on the left and clear air on the right.

Figure 5. Same as Figure 4 except for debris cloud.

Figure 6. Comparison of the average and maximum electric fields measured by ABFM-I and ABFM-II as a function of distance from cloud edge. Positive distances are outside the cloud, negative distances within. ABFM-I did not measure fields inside the cloud, and only studied active cumulus clouds. For the ABFM-II statistics the average and maximum shown here are the larger respectively of the average or maximum of either anvil or debris cloud at each distance.

FIGURES (each on separate page, with single-spaced caption)

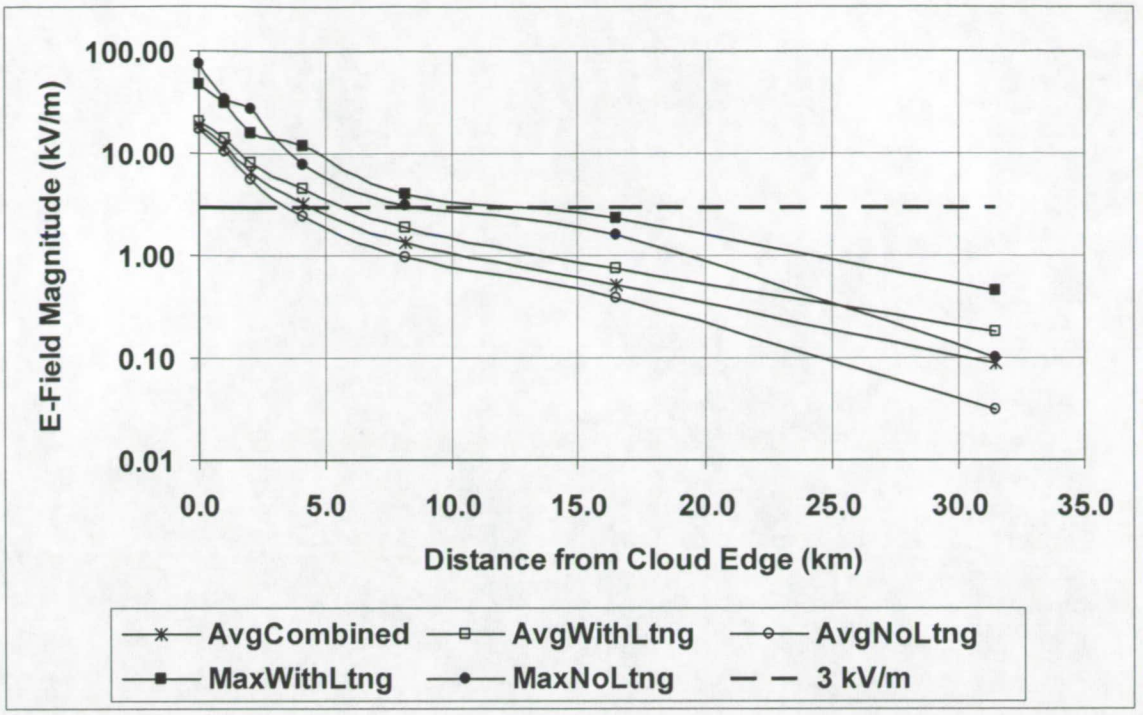

Figure 1. Electric field magnitude for ABFM - I as a function of distance from the edge of actively growing storms. In the legend, "Avg" denotes the average and "Max" denotes the peak magnitude of the field. "WithLtng" denotes storms with active lightning and "NoLtng" denotes those without active lightning at the time of sampling. The "Combined" curve includes all storms without regard for the presence of active lightning at the time of sampling.

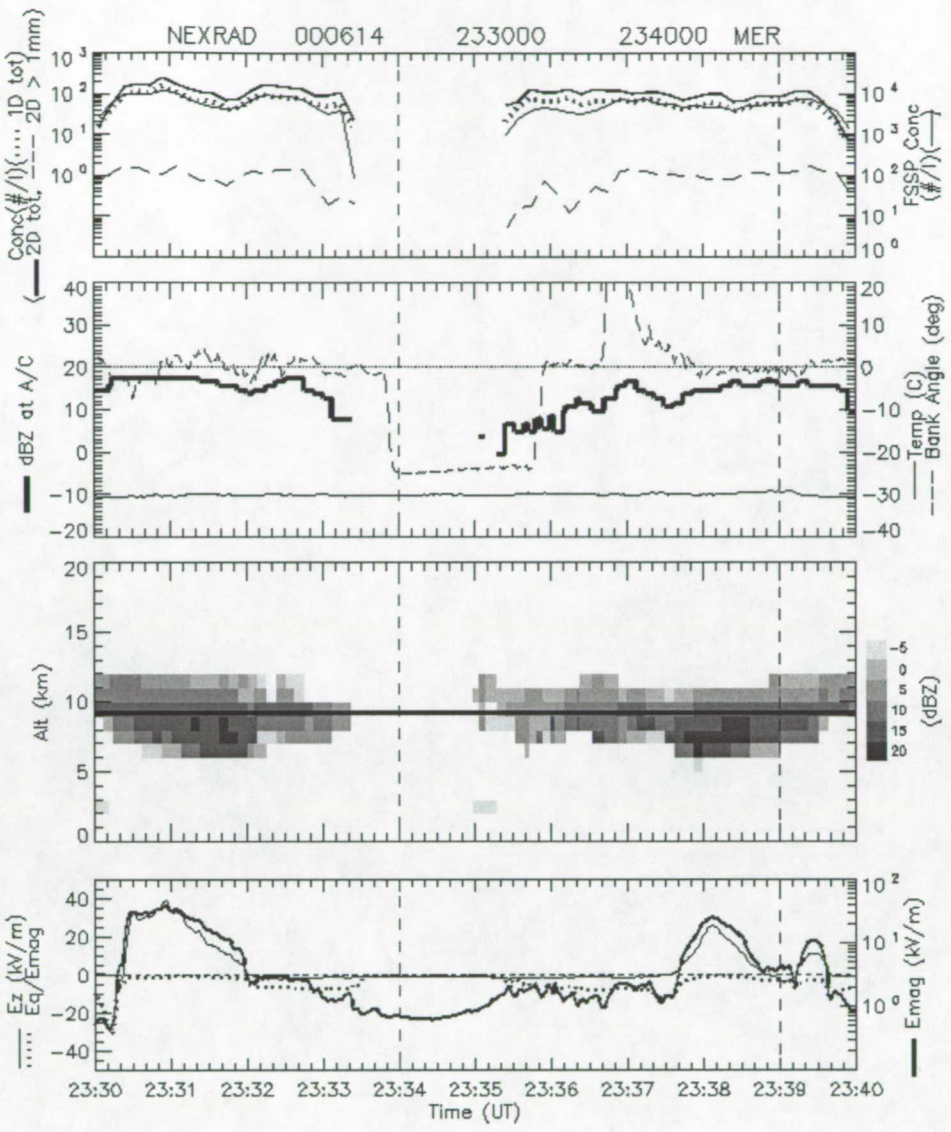

Figure 2. Typical microphysics, electric field and radar (MER) plot. The top panel shows cloud particle concentrations from the 1D, 2D and FSSP instruments. The second panel presents ground-based radar reflectivity along with the air temperature at the aircraft position plus the aircraft bank angle. The third panel is a time height presentation of ground-based radar reflectivity in a plane containing the aircraft track from the ground to the top of the radar scan. The bold line is the aircraft track. The bottom panel presents electric field components measured at the aircraft. The bold line is the scalar magnitude. The thin line is the vertical component and the dotted line is the field due to charge on the aircraft.

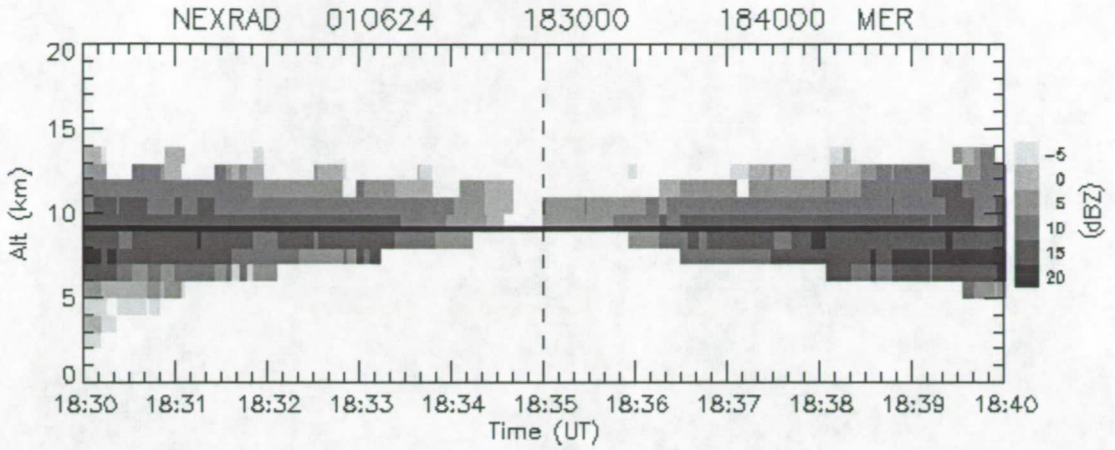

Figure 3. Radar panel of microphysics, electric field and radar (MER) plot for 24 June 2001, 1830 to 1840 UTC. Data are from the Melbourne (KMLB) WSR-88D (NEXRAD). The panel presents a vertical cross section of the reflectivity (dBZ) along the aircraft flight track. The vertical axis is altitude (km). The horizontal axis is time (UTC): each major tick represents one minute. The aircraft position is given by the solid black line near 9 km altitude. It entered the anvil one major tic to the right of center at 1835:50, but was flying less than 1 km below cloud base beginning at 1835:00 at the center of the figure.

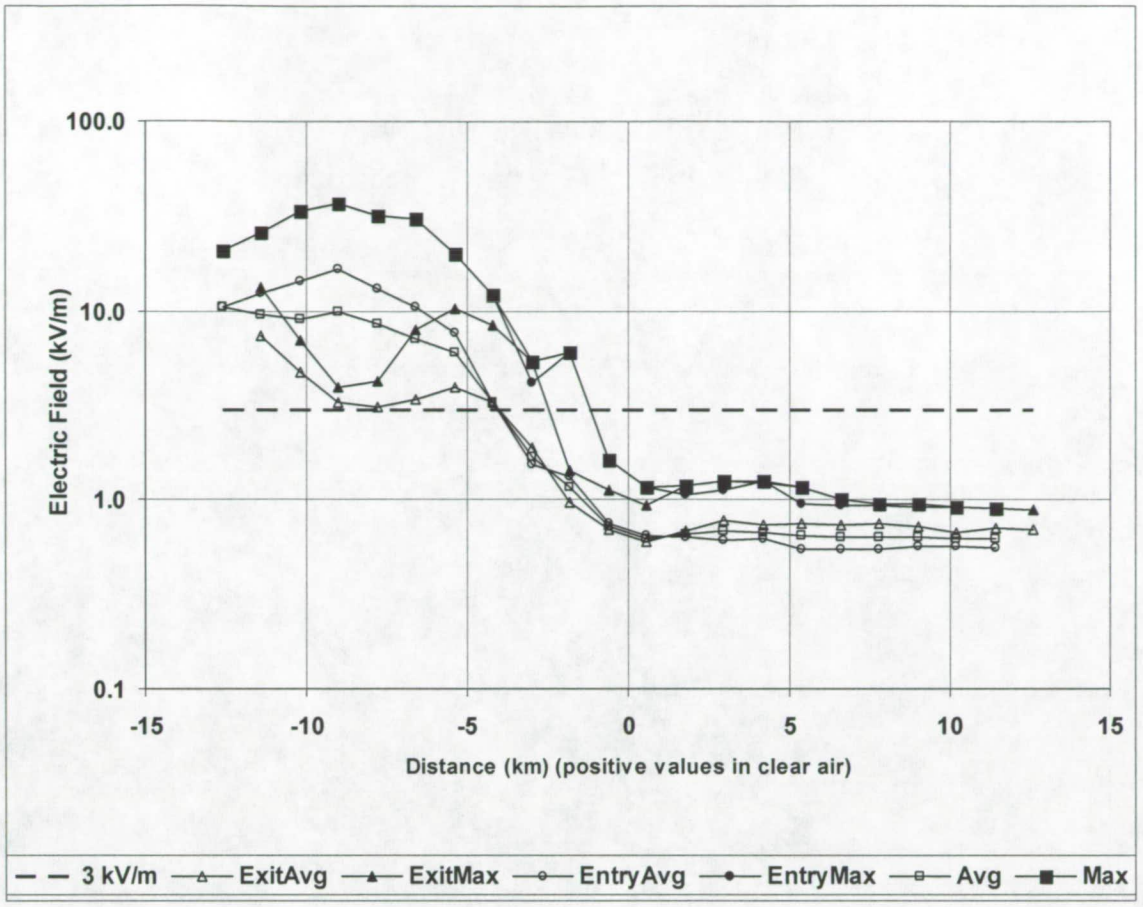

Figure 4. Electric field magnitude as a function of distance from the edge of ABFM-II anvil clouds having a maximum field magnitude of at least 3 kV m^{-1}. The maximum and average values are shown separately for passes entering cloud and exiting cloud. The hazard threshold of 3 kV m^{-1} is shown by a horizontal dashed line. The cloud boundary is at the midpoint of the chart (distance = 0) with cloud on the left and clear air on the right.

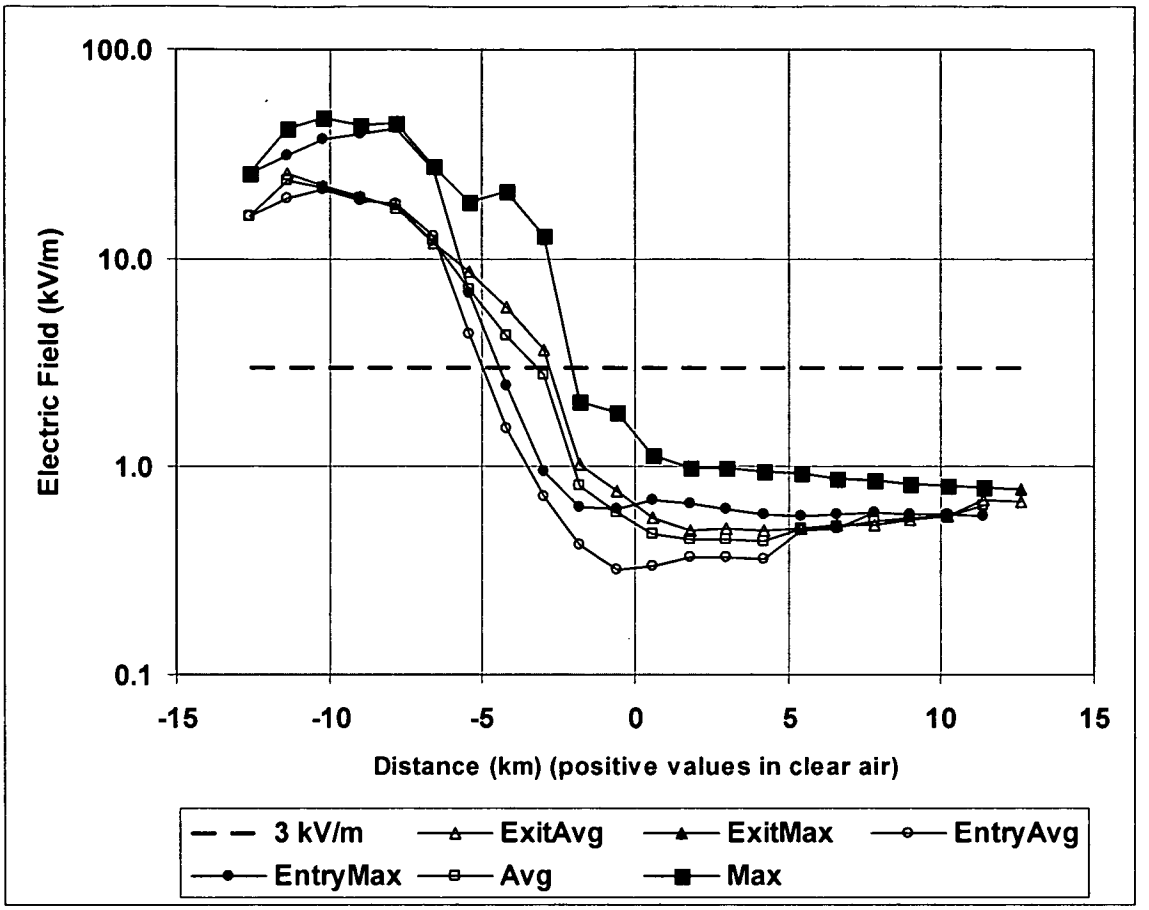

Figure 5. Same as Figure 4 except for debris cloud.

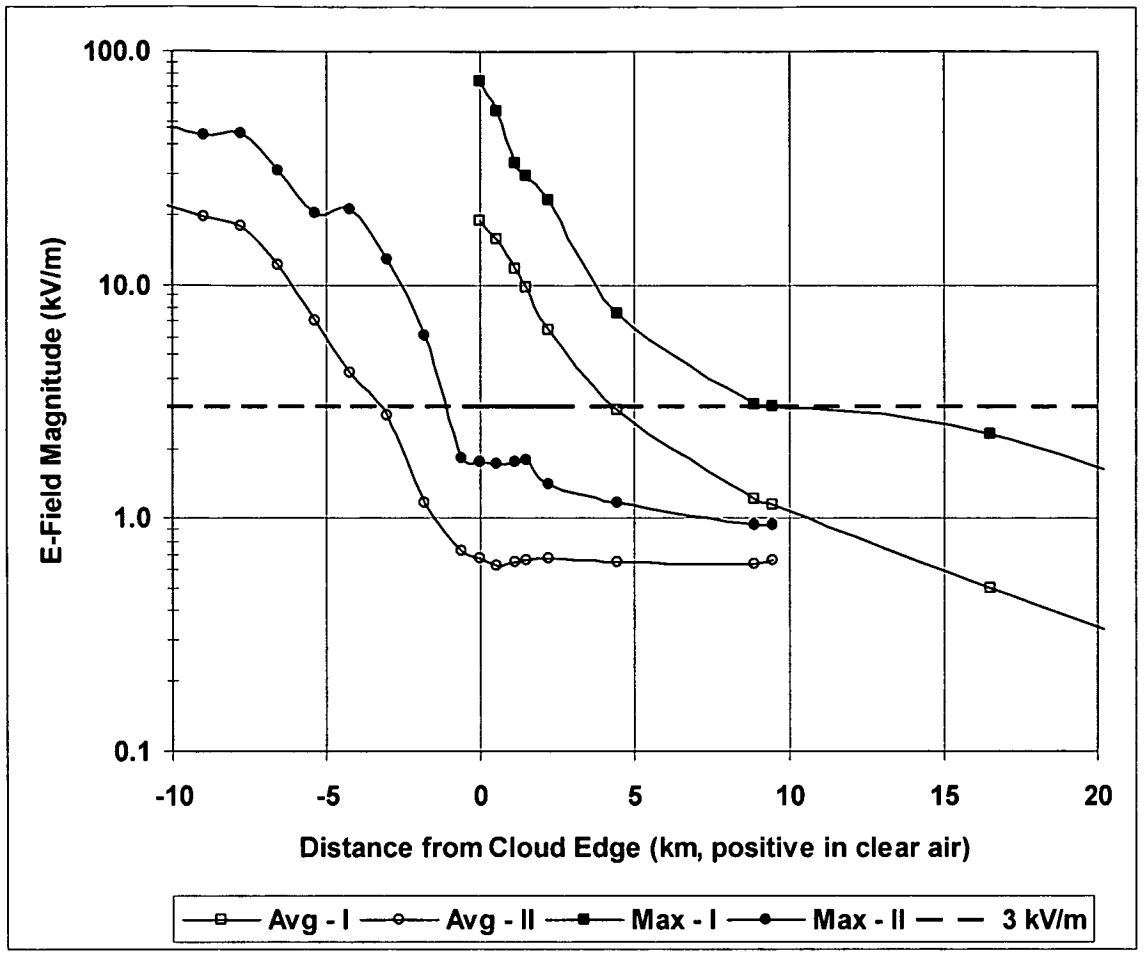

Figure 6. Comparison of the average and maximum electric fields measured by ABFM-I and ABFM-II as a function of distance from cloud edge. Positive distances are outside the cloud, negative distances within. ABFM-I did not measure fields inside the cloud, and only studied active cumulus clouds. For the ABFM-II statistics the average and maximum shown here are the larger respectively of the average or maximum of either anvil or debris cloud at each distance.